

# Detection of Steatohepatitis in a Rat Model by Using Spectroscopic Shear-Wave US Elastography<sup>1</sup>

Siavash Kazemirad, PhD Eng  
Eric Zhang, MD  
Bich N. Nguyen, MD  
Paule Bodson-Clermont, MSc  
François Destremes, PhD  
Dominique Trudel, MD, PhD  
Guy Cloutier, PhD Eng  
An Tang, MD, MSc

<sup>1</sup>From the Centre de Recherche du Centre Hospitalier de l'Université de Montréal (CRCHUM), Montreal, Quebec, Canada (S.K., E.Z., P.B.C., F.D., D.T., G.C., A.T.); Laboratory of Biorheology and Medical Ultrasonics (LBUM), Montreal, Quebec, Canada (S.K., E.Z., F.D., G.C.); Dept of Pathology, Centre Hospitalier de l'Université de Montréal (CHUM), Montreal, Quebec, Canada (B.N.N., D.T.); Dept of Pathology and Cellular Biology, Université de Montréal, Montreal, Quebec, Canada (B.N.N., D.T.); Inst of Biomedical Engineering, Université de Montréal, Montreal, Quebec, Canada (G.C.); and Dept of Radiology, Radio-oncology and Nuclear Medicine, Centre Hospitalier de l'Université de Montréal (CHUM), 1058 rue Saint-Denis, Montréal, QC, Canada H2X 3J4 (G.C., A.T.). Received February 5, 2016; revision requested March 25; revision received April 24; accepted May 20; final version accepted June 3. **Address correspondence to** A.T. (e-mail: [an.tang@umontreal.ca](mailto:an.tang@umontreal.ca)).

S.K. supported by a postdoctoral fellowship award from the Fonds de Recherche du Québec-Nature et Technologies (FRQNT). G.C. supported by Fonds Québécois de la Recherche sur la Nature et les Technologies (PR-174387) and Canadian Institutes of Health Research, Institute of Nutrition, Metabolism, and Diabetes (273738 and 301520), Quebec Bio-imaging Network (QBIN/RBIQ 5886). A.T. supported by a New Researcher Startup Grant from the Centre de Recherche du Centre Hospitalier de l'Université de Montréal and Chercheur-Boursier Junior 1 from the Fonds de Recherche du Québec en Santé and Fondation de l'Association des Radiologistes du Québec (FRQS-ARQ 26993).

© RSNA, 2016

## Purpose:

To compare low- versus high-frequency ultrasonographic (US) elastography for detection of steatohepatitis in rats by using histopathologic findings as the reference standard.

## Materials and Methods:

Between March and September 2014, after receiving approval from the institutional animal care committee, 60 male Sprague-Dawley rats were fed either a standard chow for 4 weeks or a methionine- and choline-deficient diet for 1, 4, 8, or 12 weeks to induce a continuum of steatohepatitis severity. Liver shear stiffness was assessed in vivo by using US elastography at low (40–130-Hz) and high (130–220-Hz) frequencies. Histologic features (steatosis, inflammation, and fibrosis) and modified nonalcoholic steatohepatitis categories were used as reference standards. Definite steatohepatitis was divided into steatohepatitis with fibrosis stage 1 or lower and stage 2 and higher. Analyses included the Kendall  $\tau$  correlation, multivariable linear regression analyses, Kruskal-Wallis rank sum test, and post hoc Dunn test with Holm correction.

## Results:

Correlations between liver shear stiffness and histologic features were higher at high frequencies than at low frequencies (low frequency: 0.08, 0.24, and 0.20 for steatosis, inflammation, and fibrosis, respectively; high frequency: 0.11, 0.35, and 0.50, respectively). The absolute value of multivariable regression coefficients was higher at high frequencies for the presence of steatosis, inflammation grade, and fibrosis stage (low frequency: -0.475, 0.157, and 0.209, respectively; high frequency: -0.893, 0.357, and 0.447, respectively). The model fit was better at high frequencies (adjusted  $R^2 = 0.57$ ) than at low frequencies (adjusted  $R^2 = 0.21$ ). There was a significant difference between steatohepatitis categories at both low and high frequencies ( $P = .022$  and  $P < .001$ , respectively).

## Conclusion:

Liver shear stiffness measured with US elastography provided better distinction of steatohepatitis categories at high frequencies than at low frequencies. Further, liver shear stiffness decreased with steatosis and increased with inflammation and fibrosis at both low and high frequencies.

© RSNA, 2016

Online supplemental material is available for this article.

**N**onalcoholic fatty liver disease is a highly prevalent condition identified in 20%–30% of adults in Western nations (1,2). The more advanced form, nonalcoholic steatohepatitis (NASH), is found in 3%–5% of the general population (1). If undetected and untreated, NASH may be complicated by liver fibrosis and cirrhosis. Liver biopsy is widely regarded as the reference method to grade inflammation, a hallmark feature of steatohepatitis, and to stage fibrosis, a marker of advanced liver disease (3,4). However, liver biopsy is invasive, potentially painful, and vulnerable to disease heterogeneity (5,6). Imaging-based methods may be used to potentially detect liver fat, inflammation, and fibrosis noninvasively.

Key knowledge gaps in noninvasive NASH diagnosis include the detection of inflammation, differentiation from early fibrosis, and monitoring of disease progression (4). Several magnetic resonance (MR) and ultrasonographic (US) elastography techniques

have demonstrated good to excellent diagnostic accuracy for staging of liver fibrosis (7–10). However, few studies have addressed the detection of inflammation (11–14). MR elastography studies have demonstrated a mild increase in liver stiffness with inflammation (11,12). While results of some US elastography studies suggested that liver stiffness was not associated with inflammation (13,14), recent studies have shown an increase in liver stiffness with inflammation (15,16).

The frequency of generated shear waves may influence the ability of elastography techniques to demonstrate the features of NASH. The liver has been shown to be dispersive (17), which implies that measured wave speeds and estimated mechanical properties depend on the frequency used. However, the optimum frequencies have not yet been standardized in elastography. With commercial MR elastography implementation, an external vibration frequency of 60 Hz is typically used, although frequencies between 40 and 300 Hz have been used in investigational settings (11,12,18,19). Similarly, transient US elastography, in which shear waves are generated by using external mechanical excitations, involves the use of a low excitation frequency of 50 Hz (20), whereas shear-wave US elastography techniques based on radiation pressure yielded frequencies in the range of 50–400 Hz (10,21). It is currently unclear which shear-wave frequency

range would provide better distinction between NASH categories.

The primary purpose of this study was to determine whether low-frequency or high-frequency US elastography would provide better distinction of NASH categories. The secondary purpose was to investigate the effect of steatosis, inflammation, and fibrosis on frequency-dependent liver shear stiffness.

## Materials and Methods

### Study Design and Animals

The protocol for the animal study was approved by the Institutional Animal Care Committee at the University of Montreal Hospital Research Centre. Sixty 11-week-old male Sprague-Dawley rats (Charles River Canada, Saint-Constant, Quebec, Canada) were included in this study between March and September 2014. Of those, 12 rats with free access to standard chow and water formed the control cohort and were euthanized 4 weeks after the start of the study. Forty-eight rats formed the experimental arm and were divided into four cohorts of 12 rats each, which were fed a methionine- and choline-deficient (MCD) diet (Dyets 518753; Research Diets, New Brunswick, NJ). Animals were euthanized at the time points of 1, 4, 8, and 12 weeks to obtain a range of disease severity. With the MCD diet, rats lose adipose

### Advances in Knowledge

- In an animal model of steatohepatitis, US elastography provided better distinction between histologic features (steatosis, inflammation, and fibrosis) and liver shear stiffness at high frequencies (130–220 Hz) than at low frequencies (40–130 Hz) (adjusted  $R^2$  of multivariable analysis = 0.57 and 0.21, respectively) and better distinction of steatohepatitis categories ( $P < .001$  and  $P = .022$ , respectively).
- Regression coefficient estimates at low frequencies and high frequencies demonstrated that the liver shear stiffness decreased with presence of steatosis ( $-0.475$  [ $P = .017$ ] and  $-0.893$  [ $P < .001$ ], respectively) and increased with inflammation grade ( $0.157$  [ $P = .042$ ] and  $0.357$  [ $P < .001$ ], respectively) and fibrosis stage ( $0.209$  [ $P = .004$ ] and  $0.447$  [ $P < .001$ ], respectively).

### Implications for Patient Care

- Liver shear stiffness measured with US elastography shows promise as a biomarker for noninvasive diagnosis of steatohepatitis, especially at higher shear-wave propagation frequencies.
- Steatosis should be quantified with an independent method prior to elastography-based categorization of steatohepatitis, as it mildly decreases liver shear stiffness and therefore has the potential to lead to underestimation of stiffness from inflammation and fibrosis.

### Published online before print

10.1148/radiol.2016160308 Content codes:  

Radiology 2017; 282:726–733

### Abbreviations:

MCD = methionine- and choline-deficient  
NASH = nonalcoholic steatohepatitis

### Author contributions:

Guarantor of integrity of entire study, A.T.; study concepts/study design or data acquisition or data analysis/interpretation, all authors; manuscript drafting or manuscript revision for important intellectual content, all authors; approval of final version of submitted manuscript, all authors; agrees to ensure any questions related to the work are appropriately resolved, all authors; literature research, S.K., G.C., A.T.; clinical studies, B.N.N.; experimental studies, S.K., E.Z., D.T., G.C., A.T.; statistical analysis, P.B.C.; and manuscript editing, S.K., E.Z., B.N.N., P.B.C., D.T., G.C., A.T.

Conflicts of interest are listed at the end of this article.

tissues but develop prominent steatosis, necroinflammation, and fibrosis, which resembles what is seen in human NASH (22,23).

At the end point of the study for the experimental and control cohorts, the liver was evaluated *in vivo* by means of US elastography prior to euthanasia and *ex vivo* by means of histopathologic examination after euthanasia.

### US Elastography

The rats were placed under anesthesia during preparation and US measurement phases. They were restrained in the supine position on an electric heating pad (MMHP01FFC; Mansfield Medical, Montreal, Quebec, Canada) connected to a physiological monitoring unit (THM150; VisualSonics, Toronto, Ontario, Canada) to maintain an internal temperature close to 37°C.

A shear-wave elastography beam sequence was used (24,25). Shear waves were remotely generated by a radiation force by using a linear-array US transducer (ATL L7-4; Philips, Bothell, Wash) controlled by a Verasonics system (Verasonics V1; Verasonics, Redmond, Wash). Each sequence was made of three focused pushes within the liver, spaced 4 mm apart. The US transducer excitation voltage was 40 V, and the push duration was maintained at 125  $\mu$ sec for all measurements. The tracking of shear waves was performed immediately after they were generated with the same transducer by using a fast plane wave imaging technique, which allowed acquisition of radiofrequency data at a high frame rate of 4 kHz (24). Ten consecutive pushing and tracking sequences were performed for each animal. Elastography measurements were performed by a mechanical engineer (S.K., with 6 years of experience in material characterization and elastography) who was supervised by a fellowship-trained radiologist (A.T., with 9 years of experience).

### US Data Postprocessing

Shear-wave displacement fields (as a function of time and space) were estimated from acquired radiofrequency images by using a one-dimensional

normalized cross-correlation algorithm implemented on a graphics processing unit (26). The region of interest was consistently selected on the median lobe for all animals at an approximate depth of 15 mm from the US probe. The length of the region of interest was 6–8 mm for different animals. Three reference images were acquired before the pushing phase, which were used as reference images for the estimation of displacements. Shear-wave (phase) velocities were estimated in the wave number–frequency domain, obtained by using a two-dimensional Fourier transform of the displacement field with respect to temporal and spatial coordinates (27). Liver shear stiffness values were estimated from the measured phase velocities within a frequency range of 40–220 Hz (25,28). Then the mean shear stiffness values were obtained for each animal over two frequency ranges (40–130 Hz and 130–220 Hz), which were used for statistical analyses to compare low- and high-frequency ranges.

### Histopathologic Analyses

**Liver explantation.**—The liver was explanted and fixed in a 10% formalin solution for histopathologic analysis within 4 minutes of animal euthanasia.

**Semiquantitative analysis.**—Liver specimens were subsequently stained with hematoxylin phloxine saffron stain, trichrome stain, reticulin stain, sirius red stain, and  $\alpha$ -smooth muscle actin stain (29). Pathology slides were assessed by a liver pathologist (B.N.N., with 18 years of experience) according to the NASH Clinical Research Network histologic scoring system (3). That system includes four features that are evaluated semiquantitatively: steatosis grade (grade 0–3), lobular inflammation grade (grade 0–3), hepatocellular ballooning grade (grade 0–2), and fibrosis stage (stage 0–4). Steatohepatitis categorization included “not steatohepatitis,” “borderline,” and “steatohepatitis,” on the basis of the Nonalcoholic fatty liver disease Activity Score, which is the unweighted sum of steatosis, inflammation, and ballooning grades (3). In our study, steatohepatitis was subdivided into “steatohepatitis

with fibrosis stage 1 or lower” and “steatohepatitis with fibrosis stage 2 and higher” to account for the confounding presence of fibrosis.

### Statistical Analyses

Statistical analyses were performed by using the statistical software R (version 2.10.1; R Foundation for Statistical Computing, Vienna, Austria). A *P* value less than .05 was considered to indicate a significant difference. Kendall  $\tau$  correlation was computed between liver shear stiffness and histologic features (steatosis grade, lobular inflammation grade, and fibrosis stage). The correlation coefficient was computed for liver shear stiffness measurement at low and high frequencies. To assess the confounding effect of several histopathologic changes that may coexist in steatohepatitis, we performed multivariable linear regression analyses between liver shear stiffness and histologic features at low and high frequencies. Steatosis was considered a categorical parameter, with two levels based on the absence (steatosis grade 0) or presence (steatosis grade 1–3) of macrovesicular fat, while inflammation grade and fibrosis stage were considered continuous parameters. Statistical model assumptions, including normality and heteroscedasticity, were verified. Group comparisons were performed on the basis of measured liver shear stiffness at low and high frequencies by using the nonparametric Kruskal-Wallis rank sum test between the modified steatohepatitis categories. Pairwise comparisons between groups were performed with a post hoc Dunn test with Holm correction.

To assess the confounding effect of necroinflammation and the age of animals at the time of euthanasia and to explore an exponential relationship between fibrosis and liver shear stiffness, we performed secondary multivariable regression analyses.

## Results

### Histopathologic Analyses

Histopathologic findings for the 60 rats are summarized in Table 1.

Table 1

## Histopathologic Findings in Explanted Rat Livers

Histopathologic Features	No. of Rats (n = 60)
<b>Steatosis grade</b>	
0: <5% Hepatocytes	12 (20)
1: 5%–33% Hepatocytes	1 (2)
2: 33%–66% Hepatocytes	4 (7)
3: >66% Hepatocytes	43 (72)
<b>Lobular inflammation grade</b>	
0: No foci	12 (20)
1: <2 Foci per 200× field	20 (33)
2: 2–4 Foci per 200× field	15 (25)
3: >4 Foci per 200× field	13 (22)
<b>Hepatocellular ballooning</b>	
0: None	14 (23)
1: Few balloon cells	30 (50)
2: Many cells, prominent ballooning	16 (27)
<b>Fibrosis stage</b>	
0: No fibrosis	32 (53)
1: Perisinusoidal or periportal fibrosis	21 (35)
2: Perisinusoidal and periportal fibrosis	1 (2)
3: Bridging fibrosis	4 (7)
4: Cirrhosis	2 (3)
<b>NASH diagnosis</b>	
0: Not steatohepatitis	14 (23)
1: Possible or borderline steatohepatitis	12 (20)
2a: Definite steatohepatitis with fibrosis stage 1 or lower	27 (45)
2b: Definite steatohepatitis with fibrosis stage 2 and higher	7 (12)

Note.—Numbers in parentheses are percentages.

Representative staining for each cohort is shown in Figure 1. Overall, 20% of the rats (12 of 60) had no steatosis, whereas 72% (43 of 60) had grade 3 steatosis. A relatively even distribution of lobular inflammation grade was observed: 20% of rats (12 of 60) had grade 0, 33% of rats (20 of 60) had grade 1, 25% of rats (15 of 60) had grade 2, and 22% of rats (13 of 60) had grade 3. Fifty-three of 60 rats (88%) developed no or mild fibrosis (stage 0 or 1), and seven rats (12%) developed fibrosis of stage 2 and higher. Fourteen of 60 rats (23%) were categorized as “not steatohepatitis,” 20% (12 of 60) were in the borderline category, 45% (27 of 60) had steatohepatitis with fibrosis stage 1 or lower, and 12% (seven of 60) developed steatohepatitis with fibrosis stage 2 and higher.

Distributions of histologic scoring for each cohort are shown in Figure 2.

Macrovesicular fat was observed in most hepatocytes after 1 week of MCD diet consumption, where the mean steatosis grade  $\pm$  standard deviation was  $2.5 \pm 0.7$  and reached a maximum after 4 weeks. Lobular inflammation grade was lowest in the control cohort at  $0.3 \pm 0.5$ , increased initially with the duration of MCD diet consumption, reached a peak value at 8 weeks, and decreased at 12 weeks. Fibrosis was absent (stage 0) in all rats in the control cohort and the 1-week MCD cohort. Mild fibrosis (stage 1) was observed in four rats in the 4-week cohort, whereas all the rats in the 8-week and 12-week cohorts developed mild to severe fibrosis (stage 1–4).

### Correlation Analyses

Correlation coefficients between liver shear stiffness and histologic features were higher at high frequencies than at

low frequencies (Table 2). Lobular inflammation grade and fibrosis stage presented the strongest associations with liver shear stiffness at high frequencies (moderate correlation,  $\tau = 0.35$  [ $P < .001$ ] and  $\tau = 0.50$  [ $P < .001$ ], respectively). Similar results were observed at low frequencies, however, with a lower correlation.

### Multivariable Analyses

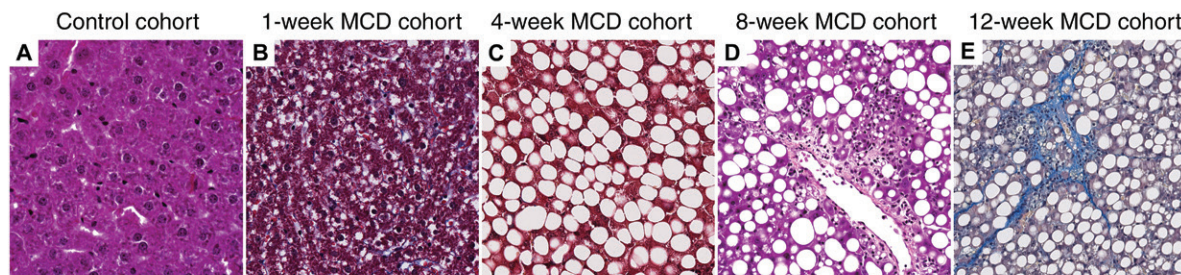
In the multivariable analysis, conducted by using histologic features as independent variables, the regression coefficient estimates demonstrated that the liver shear stiffness decreased with presence of steatosis (negative estimates) and increased with inflammation grade and fibrosis stage (positive estimates), at both low frequencies and high frequencies (Table 3). The absolute value of the regression coefficient estimates for presence of steatosis, inflammation grade, and fibrosis stage was higher at high frequencies ( $-0.893$ ,  $0.357$ , and  $0.447$ , respectively) than at low frequencies ( $-0.475$ ,  $0.157$ , and  $0.209$ , respectively).

Keeping all other variables constant, the effects of presence of steatosis, inflammation grade, and fibrosis stage were all significant at low frequencies ( $P = .017$ ,  $P = .042$ , and  $P = .004$ , respectively) and at high frequencies (all  $P < .001$ ).

The multivariable regression models with histologic features provided a better fit to the experimentally obtained shear stiffness values at high frequencies (adjusted  $R^2 = 0.57$ ) than at low frequencies (adjusted  $R^2 = 0.21$ ). This indicates that the regression models with histologic features could be used to explain 57% of the total variance of high-frequency elastography and only 21% of the variance of low-frequency elastography.

The multivariable regression coefficient estimates obtained at high frequencies were approximately twice the estimates obtained at low frequencies, with relative errors of 4%, 6%, 13%, and 7% for the intercept, presence of steatosis, inflammation grade, and fibrosis stage, respectively. The standard errors were of the same order of

**Figure 1**



Mean Shear Stiffness (kPa)	Control cohort	1-week MCD cohort	4-week MCD cohort	8-week MCD cohort	12-week MCD cohort
40-130 Hz	1.67 kPa	1.20 kPa	1.66 kPa	1.70 kPa	1.87 kPa
130-220 Hz	3.47 kPa	2.67 kPa	3.16 kPa	3.84 kPa	4.27 kPa

**Figure 1:** Photomicrographs (original magnification,  $\times 20$ ) in an animal model of NASH with, A, D, hematoxylin-eosin stain and, B, C, E, trichrome stain. The Sprague-Dawley control rats were fed a standard chow or an MCD diet for 1, 4, 8, or 12 weeks to induce a continuum of NASH severity. The onset of steatosis can be seen at 1 week with progressive increase of steatosis thereafter, as well as marked increase of inflammation at 8 weeks and fibrosis at 12 weeks.

**Figure 2**

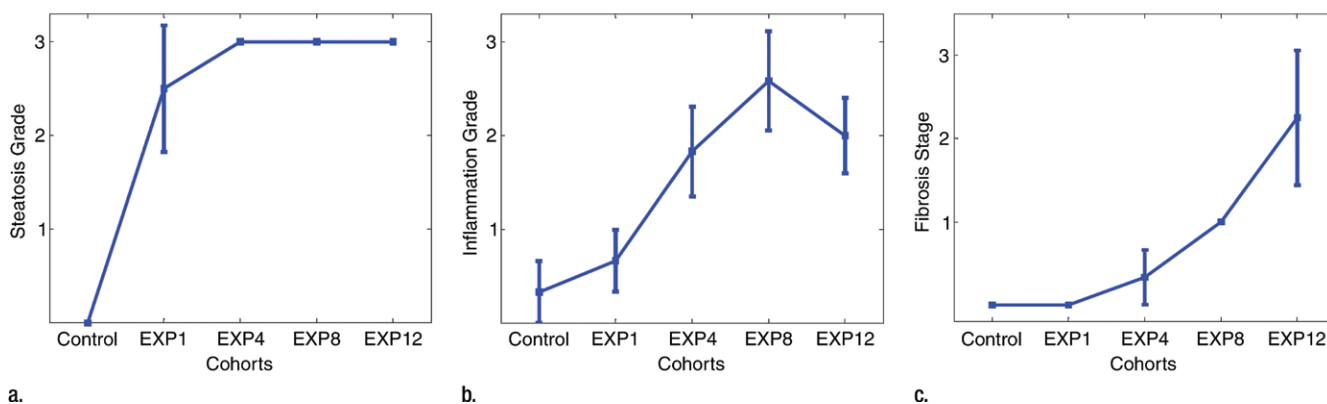


**Figure 2:** Plots show histologic grading (mean  $\pm$  standard deviation) results according to semiquantitative analysis between cohorts for (a) steatosis grade, (b) inflammation grade, and (c) fibrosis stage. All the animals in the control cohort and in the 4-week, 8-week, and 12-week cohorts had the same steatosis grade, and all the animals in the control cohort and the 1-week and 8-week cohorts had the same fibrosis stage. Therefore, the standard deviation of these histologic features was zero for the corresponding cohorts. EXP1 = 1-week experimental cohort, EXP4 = 4-week experimental cohort, EXP8 = 8-week experimental cohort, EXP12 = 12-week experimental cohort.

magnitude at high and low frequencies, with corresponding relative errors of 5%, 5%, 4%, and 4%, respectively.

**Comparison of Steatohepatitis Categories**

At low frequencies, liver shear stiffness was significantly different ( $P = .022$ ) between the steatohepatitis categories (Fig 3). However, post hoc tests only demonstrated higher liver stiffness in steatohepatitis with fibrosis stage 2 and higher compared with borderline steatohepatitis ( $P = .023$ ).

At high frequencies, liver shear stiffness was significantly different ( $P$

**Table 2**

**Results of Kendall  $\tau$  Correlation between Liver Shear Stiffness and Histologic Features at Low and High Frequencies**

Histologic Features	Low Frequency (40–130 Hz)	High Frequency (130–220 Hz)
Steatosis grade	0.08 ( $P = .477$ )	0.11 ( $P = .306$ )
Lobular inflammation grade	0.24 ( $P = .014$ )	0.35 ( $P < .001$ )
Fibrosis stage	0.20 ( $P = .057$ )	0.50 ( $P < .001$ )

$< .001$ ) between steatohepatitis categories. Post hoc tests demonstrated higher stiffness values (a) for “not steatohepatitis” than for borderline steatohepatitis ( $P = .034$ ), (b) for

steatohepatitis with fibrosis stage 1 or lower than for borderline steatohepatitis ( $P = .002$ ), and (c) for steatohepatitis with fibrosis stage 2 and higher than for “not steatohepatitis” ( $P = .005$ ),

Table 3

## Results of Multivariable Analysis

Frequency Range and Parameter	Estimate	Standard Error	P Value	Adjusted R <sup>2</sup> Value
40–130 Hz				0.21
Intercept	1.615	0.142	<.001	...
Presence of steatosis	−0.475	0.192	.017	...
Lobular inflammation grade	0.157	0.076	.042	...
Fibrosis stage	0.209	0.069	.004	...
130–220 Hz				0.57
Intercept	3.349	0.149	<.001	...
Presence of steatosis	−0.893	0.201	<.001	...
Lobular inflammation grade	0.357	0.079	<.001	...
Fibrosis stage	0.447	0.072	<.001	...

borderline steatohepatitis ( $P < .001$ ), or steatohepatitis with fibrosis stage 1 or lower ( $P = .018$ ).

### Secondary Analyses

The results of the secondary analyses are presented and discussed in Appendix E1 (online).

### Discussion

We have shown that liver shear stiffness decreased with steatosis and increased with inflammation or fibrosis. To be able to generalize the results obtained for the effect of steatosis on liver shear stiffness, steatosis was considered a categorical parameter in the multivariable regression analyses. There were 12 animals with grade 0 steatosis (control animals) and 43 animals with grade 3 steatosis. Therefore, the results of the multivariable analyses are reliably applied to the effect of severe steatosis on liver stiffness, especially at high frequencies ( $P < .001$ ). Liver shear stiffness was significantly different between groups of rats categorized according to steatohepatitis diagnosis, at both low and high frequencies. However, we found that frequencies between 130 and 220 Hz provided better distinction of steatohepatitis categories than did the lower frequencies.

The fact that the multivariable regression coefficient estimates obtained at high frequencies were approximately twice the estimates obtained at low frequencies indicates that the relative

effect of these features was approximately the same over the two frequency ranges. However, standard errors were of the same order of magnitude at high and low frequencies. Moreover, the regression with histologic features was used to explain a substantially larger amount of variance at high frequencies than at low frequencies. Therefore, the discrimination power at high frequencies was better than at low frequencies. This means that tendencies of the effects of parameters, and thus differences between liver shear stiffness of different steatohepatitis categories, might be easier to observe at high frequencies. Liver shear stiffness values obtained for different steatohepatitis categories were higher in the high frequency range. These results are consistent with prior observations by Klatt et al, who demonstrated highly dispersive liver with oscillatory rheometry and multifrequency MR elastography (17). The frequency-dependent shear stiffness of soft biomaterials and tissues depends on the configurational rearrangements of neighboring microstructures that occur during dynamic loading (30). Since all histologic features of NASH do not influence the microstructures and thus the frequency-dependent liver stiffness in the same way, the changes in the stiffness of different steatohepatitis categories with respect to frequency may be different. This may further explain why the ability to distinguish between steatohepatitis categories may be better at higher frequency ranges.

The effect of steatosis on liver stiffness remains controversial in the literature. While some MR elastography studies performed at low frequency (typically 60 Hz) did not demonstrate any significant effect of fat on liver stiffness (31–33), a US elastography clinical study performed by Yoneda et al showed lower stiffness values in patients with simple steatosis compared with healthy volunteers (13). Our results suggest that prior discrepancies regarding the effect of fat on liver stiffness may be explained by different frequency ranges used in these studies. Further, the decrease in liver stiffness of the borderline category with respect to the “not steatohepatitis” category may be explained by the confounding presence of steatosis. As shown by the results of our multivariable analysis, the stiffness-lowering effect of fat is more apparent at high frequencies.

Inflammation may also change the tissue stiffness, although its effect has not been made clear in prior literature. In human studies of US elastography, Yoneda et al (13) and Palmeri et al (14) did not find a correlation between liver shear stiffness and inflammation, whereas Zeng et al (15) and Dong et al (16) reported a mild increase in liver shear stiffness with inflammation grade. Georges et al (29) also found that inflammation did not explain increased liver shear stiffness ex vivo according to rheology measurements of rat livers. However, Chen et al (12) reported significantly higher stiffness values for patients with inflammation compared with those with simple steatosis by using MR elastography. Inflammation may cause edema (34), thus increasing the internal pressure of the liver and therefore liver stiffness. This observation is in agreement with our results, as we observed an increase in liver stiffness with inflammation.

The effect of fibrosis on liver shear stiffness has been extensively investigated in the literature by using both US (10,13,14) and MR elastography (11,12,31,32,35). These studies have shown a significant increase in liver shear stiffness with higher fibrosis stages. This is also in agreement with

Figure 3

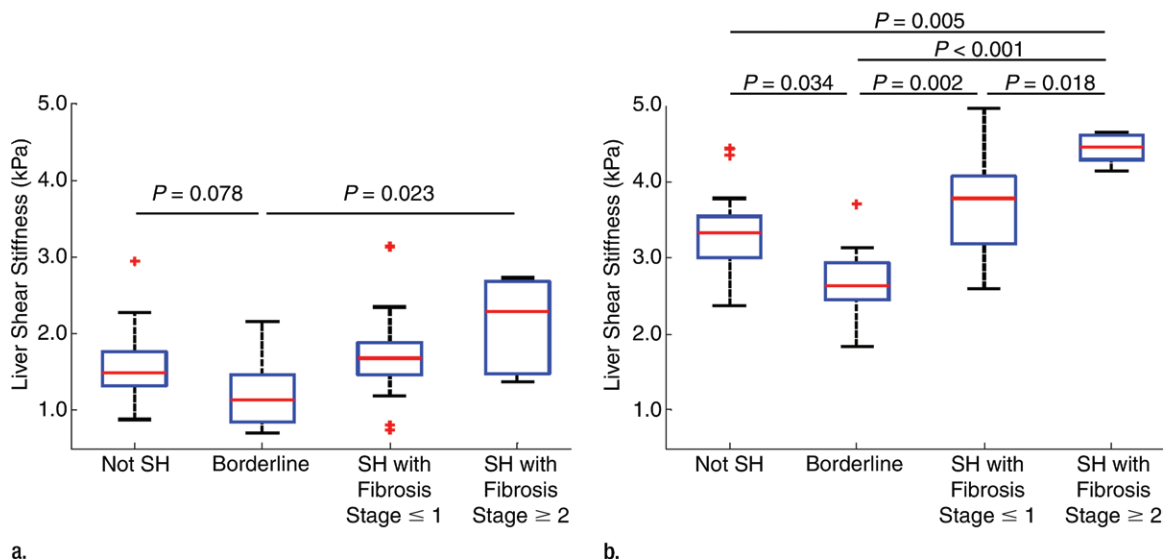


**Figure 3:** Box and whisker plots demonstrate liver shear stiffness measured at (a) low frequencies (40–130 Hz) and (b) high frequencies (130–220 Hz). SH = steatohepatitis.

the higher shear stiffness values we observed in the steatohepatitis with fibrosis stage 2 and higher category compared with the other steatohepatitis categories.

Another potential source of discrepancies in prior literature may be the confounding effects of steatosis, inflammation, and fibrosis in the NASH continuum on liver stiffness. The coexistence of these conditions may explain the lack of correlations between the liver shear stiffness and histologic findings. However, a relatively good fit was obtained at high frequencies between the multivariable linear regression models and measured liver shear stiffness values, demonstrating the effect of each histologic feature on liver shear stiffness when the confounding effect of the other features was taken into account.

Like most current US elastography methods, a limitation of our study was that we only assessed elasticity and did not provide spectroscopic measurement of viscosity. One potential approach to obtain viscosity measurements is to fit a rheological model to the measured shear wave speeds. Accounting for viscosity did not significantly improve the performance of elasticity in liver fibrosis staging according to Chen et al (10).

Further research should be conducted to investigate whether viscoelasticity would improve the distinction of NASH disease categories.

In this study, the animals in the control cohort had grade 0 steatosis, and most of the animals in the experimental cohorts had grade 3 steatosis. Modification of the diet composition may be required to obtain milder steatosis grades in future studies focused on the effect of early steatosis on mechanical properties of liver.

The two categories of “not steatohepatitis” and steatohepatitis with fibrosis stage of 1 or lower could not be separated by using elastography alone because the stiffness-lowering effect of liver steatosis was superposed with the stiffness-increasing effect of inflammation and fibrosis. In this study, we focused on assessment of liver stiffness and did not assess other quantitative US parameters, such as attenuation or backscatter coefficients (36,37). We anticipate that a two-step diagnostic approach that includes an independent method for fat quantification prior to elastography assessment of the liver may further improve classification of steatohepatitis categories.

In conclusion, this animal study based on an MCD dietary model of

steatohepatitis helps to identify the frequency range that permits better distinction of steatohepatitis categories. In our study, liver shear stiffness provided better distinction between steatohepatitis categories at high frequencies than at low frequencies; moreover, multivariable analysis demonstrated that liver shear stiffness decreased with steatosis and increased with inflammation and fibrosis at both low and high frequencies. These results suggest that in future studies, shear-wave frequency should be taken into account to improve the classification accuracy in NASH. Future work may be conducted to explore a broader range of frequencies, although very high frequencies may be difficult to achieve in humans because of the dissipative nature of soft tissues, which affects the high-frequency components of shear waves more.

**Disclosures of Conflicts of Interest:** S.K. disclosed no relevant relationships. E.Z. disclosed no relevant relationships. B.N.N. disclosed no relevant relationships. P.B.C. disclosed no relevant relationships. F.D. disclosed no relevant relationships. D.T. disclosed no relevant relationships. G.C. Activities related to the present article; disclosed no relevant relationships. Activities not related to the present article: author received payment from Acist Medical Systems for consulting. Other relationships: disclosed no relevant relationships. A.T. disclosed no relevant relationships.

## References

- Vernon G, Baranova A, Younossi ZM. Systematic review: the epidemiology and natural history of non-alcoholic fatty liver disease and non-alcoholic steatohepatitis in adults. *Aliment Pharmacol Ther* 2011;34(3):274–285.
- Zhang E, Wartelle-Bladou C, Lepanto L, Lachaine J, Cloutier G, Tang A. Cost-utility analysis of nonalcoholic steatohepatitis screening. *Eur Radiol* 2015;25(11):3282–3294.
- Kleiner DE, Brunt EM, Van Natta M, et al. Design and validation of a histological scoring system for nonalcoholic fatty liver disease. *Hepatology* 2005;41(6):1313–1321.
- Sanyal AJ, Brunt EM, Kleiner DE, et al. Endpoints and clinical trial design for non-alcoholic steatohepatitis. *Hepatology* 2011;54(1):344–353.
- Ratziu V, Charlotte F, Heurtier A, et al. Sampling variability of liver biopsy in non-alcoholic fatty liver disease. *Gastroenterology* 2005;128(7):1898–1906.
- Fernández-Salazar L, Velayos B, Aller R, Lozano F, Garrote JA, González JM. Percutaneous liver biopsy: patients' point of view. *Scand J Gastroenterol* 2011;46(6):727–731.
- Singh S, Venkatesh SK, Wang Z, et al. Diagnostic performance of magnetic resonance elastography in staging liver fibrosis: a systematic review and meta-analysis of individual participant data. *Clin Gastroenterol Hepatol* 2015;13(3):440–451.e6.
- Friedrich-Rust M, Ong MF, Martens S, et al. Performance of transient elastography for the staging of liver fibrosis: a meta-analysis. *Gastroenterology* 2008;134(4):960–974.
- Friedrich-Rust M, Nierhoff J, Lupsor M, et al. Performance of acoustic radiation force impulse imaging for the staging of liver fibrosis: a pooled meta-analysis. *J Viral Hepat* 2012;19(2):e212–e219.
- Chen S, Sanchez W, Callstrom MR, et al. Assessment of liver viscoelasticity by using shear waves induced by ultrasound radiation force. *Radiology* 2013;266(3):964–970.
- Salameh N, Larrat B, Abarca-Quinones J, et al. Early detection of steatohepatitis in fatty rat liver by using MR elastography. *Radiology* 2009;253(1):90–97.
- Chen J, Talwalkar JA, Yin M, Glaser KJ, Sanderson SO, Ehman RL. Early detection of nonalcoholic steatohepatitis in patients with nonalcoholic fatty liver disease by using MR elastography. *Radiology* 2011;259(3):749–756.
- Yoneda M, Suzuki K, Kato S, et al. Nonalcoholic fatty liver disease: US-based acoustic radiation force impulse elastography. *Radiology* 2010;256(2):640–647.
- Palmeri ML, Wang MH, Rouze NC, et al. Noninvasive evaluation of hepatic fibrosis using acoustic radiation force-based shear stiffness in patients with nonalcoholic fatty liver disease. *J Hepatol* 2011;55(3):666–672.
- Zeng X, Xu C, He D, et al. Influence of hepatic inflammation on FibroScan findings in diagnosing fibrosis in patients with chronic hepatitis B. *Ultrasound Med Biol* 2015;41(6):1538–1544.
- Dong DR, Hao MN, Li C, et al. Acoustic radiation force impulse elastography, FibroScan, Forns' index and their combination in the assessment of liver fibrosis in patients with chronic hepatitis B, and the impact of inflammatory activity and steatosis on these diagnostic methods. *Mol Med Rep* 2015;11(6):4174–4182.
- Klatt D, Friedrich C, Korth Y, Vogt R, Braun J, Sack I. Viscoelastic properties of liver measured by oscillatory rheometry and multifrequency magnetic resonance elastography. *Biorheology* 2010;47(2):133–141.
- Asbach P, Klatt D, Schlosser B, et al. Viscoelasticity-based staging of hepatic fibrosis with multifrequency MR elastography. *Radiology* 2010;257(1):80–86.
- Huwart L, Sempoux C, Salameh N, et al. Liver fibrosis: noninvasive assessment with MR elastography versus aspartate aminotransferase-to-platelet ratio index. *Radiology* 2007;245(2):458–466.
- Sandrin L, Fourquet B, Hasquenoph JM, et al. Transient elastography: a new noninvasive method for assessment of hepatic fibrosis. *Ultrasound Med Biol* 2003;29(12):1705–1713.
- Muller M, Gennisson JL, Defieux T, Tanter M, Fink M. Quantitative viscoelasticity mapping of human liver using supersonic shear imaging: preliminary in vivo feasibility study. *Ultrasound Med Biol* 2009;35(2):219–229.
- Rinella ME, Elias MS, Smolak RR, Fu T, Borensztajn J, Green RM. Mechanisms of hepatic steatosis in mice fed a lipogenic methionine choline-deficient diet. *J Lipid Res* 2008;49(5):1068–1076.
- Hebbard L, George J. Animal models of nonalcoholic fatty liver disease. *Nat Rev Gastroenterol Hepatol* 2011;8(1):35–44.
- Bercoff J, Tanter M, Fink M. Supersonic shear imaging: a new technique for soft tissue elasticity mapping. *IEEE Trans Ultrason Ferroelectr Freq Control* 2004;51(4):396–409.
- Ouared A, Montagnon E, Kazemirad S, Gaboury L, Robidoux A, Cloutier G. Frequency adaptation for enhanced radiation force amplitude in dynamic elastography. *IEEE Trans Ultrason Ferroelectr Freq Control* 2015;62(8):1453–1466.
- Ophir J, Céspedes I, Ponnekanti H, Yazdi Y, Li X. Elastography: a quantitative method for imaging the elasticity of biological tissues. *Ultrason Imaging* 1991;13(2):111–134.
- Bernal M, Nenadic I, Urban MW, Greenleaf JF. Material property estimation for tubes and arteries using ultrasound radiation force and analysis of propagating modes. *J Acoust Soc Am* 2011;129(3):1344–1354.
- Sandrin L, Tanter M, Catheline S, Fink M. Shear modulus imaging with 2-D transient elastography. *IEEE Trans Ultrason Ferroelectr Freq Control* 2002;49(4):426–435.
- Georges PC, Hui JJ, Gombos Z, et al. Increased stiffness of the rat liver precedes matrix deposition: implications for fibrosis. *Am J Physiol Gastrointest Liver Physiol* 2007;293(6):G1147–G1154.
- Lakes R. *Viscoelastic materials*. New York, NY: Cambridge University Press, 2009.
- Yin M, Talwalkar JA, Glaser KJ, et al. Assessment of hepatic fibrosis with magnetic resonance elastography. *Clin Gastroenterol Hepatol* 2007;5(10):1207–1213.e2.
- Lee YJ, Lee JM, Lee JE, et al. MR elastography for noninvasive assessment of hepatic fibrosis: reproducibility of the examination and reproducibility and repeatability of the liver stiffness value measurement. *J Magn Reson Imaging* 2014;39(2):326–331.
- Venkatesh SK, Wang G, Teo LL, Ang BW. Magnetic resonance elastography of liver in healthy Asians: normal liver stiffness quantification and reproducibility assessment. *J Magn Reson Imaging* 2014;39(1):1–8.
- Iredale JP. Models of liver fibrosis: exploring the dynamic nature of inflammation and repair in a solid organ. *J Clin Invest* 2007;117(3):539–548.
- Loomba R, Wolfson T, Ang B, et al. Magnetic resonance elastography predicts advanced fibrosis in patients with nonalcoholic fatty liver disease: a prospective study. *Hepatology* 2014;60(6):1920–1928.
- Sasso M, Beaugrand M, de Ledinghen V, et al. Controlled attenuation parameter (CAP): a novel VCTE guided ultrasonic attenuation measurement for the evaluation of hepatic steatosis: preliminary study and validation in a cohort of patients with chronic liver disease from various causes. *Ultrasound Med Biol* 2010;36(11):1825–1835.
- Lin SC, Heba E, Wolfson T, et al. Noninvasive diagnosis of nonalcoholic fatty liver disease and quantification of liver fat using a new quantitative ultrasound technique. *Clin Gastroenterol Hepatol* 2015;13(7):1337–1345.e6.